IEEE Access
Multidisciplinary | Rapid Review | Open Access Journal

Received December 6, 2019, accepted December 24, 2019, date of publication December 30, 2019, date of current version January 8, 2020.

Digital Object Identifier 10.1109/ACCESS.2019.2962917

Fabric Pilling Hairiness Extraction From Depth Images Based on the Predicted Fabric Surface Plane

CHAO ZHI, ZHONG-YUAN GAO, GUAN-LIN WANG, MENG-QI CHEN, WEI FAN, AND LING-JIE YU, (Member, IEEE)
School of Textile Science and Engineering, Xi'an Polytechnic University, Xi'an 710048, China

Corresponding author: Ling-Jie Yu (lingjie.yu@xpu.edu.cn)

This work was supported in part by the National Natural Science Foundation of China under Grant 51903199 and Grant 51603163, in part by the Science and Technology Project of Shaanxi Province under Grant 2018JQ5214, Grant 2019JQ-182, and Grant 2017JQ5056, and in part by the Scientific Research Program Funded by Shaanxi Provincial Education Department under Grant 18JS039.

ABSTRACT A new approach for extracting the hairiness from fabric based on the predicted fabric surface plane is presented in this paper to extract the hairiness from the depth image. The depth from focus (DFF) technique is utilized in this study to establish the depth image of the pilled fabrics by using a series of image layers captured under a microscope. A pilled fabric depth image provides information on the hairiness and the fabric surface, and the hairiness is located above the fabric surface. However, the depth value of the fabric surface covered with hairiness cannot be directly obtained. Therefore, for hairiness extraction, a predicted plane of the fabric surface is fitted by selecting several base points on the fabric surface. The target above the predicted plane will be considered as hairiness and will be extracted. The oversegmentation method based on the mean shift algorithm is used in the study to select the base points of the fabric surface. First, several seed points are marked along the Sobel edges; then, several oversegmented areas are formed after the growth of the seed points, which are called split pieces in this paper. The split pieces of the fabric surfaces are selected as the base points according to the depth value as well as the spatial direction of each split piece. Finally, the predicted plane of the fabric surface is established using these base points. The results of significance testing show that is it reasonable to assume that the fabric surface can be expressed as a plane. The results of the residual examination show that the predicted plane can correctly calculate the depth value (z) of the fabric surface at any plane position (x, y). The extracted hairiness images show that hairiness can be correctly and completely obtained through the predicted plane.

INDEX TERMS Object segmentation, surface fitting, hairiness extraction, pilling assessment, automatic testing.

I. INTRODUCTION

Pilling ruins the original appearance of a fabric. Normally, the pilling grade of a fabric is assessed through manual observation by comparing the sample with standard pilling photographs. This subjective method can be incorrect and inconsistent since the evaluator's experience, psychology and physiology may affect the correctness of the assessment result [1].

To overcome the above problems, an objective method using image processing has been reported [2]. A pilled fabric image includes both the fabric surface pattern, the hairiness, the pills and the illumination. The key difficulties in objective pilling evaluation are the extraction of the hairiness and pills from the fabric surface pattern. Many researchers have tried to separate the hairiness and pills from the background by image analysis techniques. Furferi *et al.* [3] devised a machine vision-based procedure with the aim of extracting a number of parameters that characterize the fabric. These parameters were then used to train an artificial neural network to automatically grade the fabrics in terms of pilling. Yang *et al.* [4] proposed the use of deep principal components analysis-based neural networks (DPCANNs) for fabric pilling identification. Guan *et al.* [5] developed an

The associate editor coordinating the review of this manuscript and approving it for publication was Kumaradevan Punithakumar.

objective evaluation method by forming multiscale filtering images with Gaussian pyramid decomposition, building a saliency map with a center-surround difference algorithm and extracting the pilling feature. Deng *et al.* [6] proposed a new approach for hairiness and pills extraction based on the multiscale two-dimensional dual-tree complex wavelet transform (CWT). Lee and Lin [7] devised an integrated computer vision and type-2 hairiness cerebellar model articulation controller (T2FCMAC) to classify the pilling of knitted fabric. Eldessouki and Hassan [8] described an algorithm for creating a features dataset for training and testing the soft-computing classifier, where random noise was added to the limited number of the fabric's pilling standard images.

Fabrics can exhibit complex patterns; thus, while image analysis techniques using 2D images can be effective for fabrics with periodic textures, they may not be suitable for fabrics with unregular patterns [6]. Many researchers have tried to extract hairiness and pills using 3D images. Techniková *et al.* [9] reconstructed a 3D fabric surface image from shading based on a gradient field method. Xu *et al.* [10] used two parallel-placed digital cameras to capture binocular images in order to establish the image surface and then described the local features of the images. Wang *et al.* [11] also adopted a stereovision system to generate the 3D image.

A pilled fabric often has distinct pills as well as ambiguous hairiness and small pills that are difficult to classify [6]. Hairiness is often on the order of microns in width. Therefore, a microscope is used to magnify the fabric. However, the microscope cannot directly obtain the depth information of the fabric surface. Many researchers have utilized the Depth from Focus (DFF) method to calculate the depth value of the sample surface [12], [13]. In a previous study, a depth image of a pilled fabric was reconstructed. In this paper, a method of extracting the hairiness from fabric images based on depth information is proposed.

II. METHOD

A. SAMPLE PREPARATION

Fabrics have five levels of pilling according to the standard GB/T 4802.1-2008. pilling grade 1 refers to the fabrics with severe pills and hairiness, and pilling grade 5 refers to fabrics with few pills and hairiness. Five fabrics varying from pilling grade 1 to pilling grade 5 were used to explore the segmentation method.

The five fabrics contain both knitting and weaving with different colors. The density of the knitting fabrics can be expressed by the course density (which refers to the number of wales every 5 cm) and the wale density (which refers to numbers of courses every 5 cm). The density of weaving fabrics can be described by the weft density (which refers to the number of weft yarns every 10 cm) and the warp density (which refers to the number of warp yarns every 10 cm). In this study, the wale density of the knitting fabrics was between 60 courses/ (5 cm) and 80 courses/ (5 cm), and the course density were between 70 wales/ (5 cm) and 90 wales/ (5 cm). The weft density was between 300 yarns/ (10 cm) and 360 yarns/ (10 cm), and the warp density of the weaving fabrics was between 230 yarns/ (10 cm) and 290 yarns/ (10 cm).

An automatic microscope (M318, BEION Co., Ltd, Shanghai, China) was used to obtain the sequential images of these fabrics. By moving the objective stage along the z-axis, a series of multifocused images was captured at each step. The scale of the images captured are 800 pixels × 600 pixels, for which one pixel is 2.16 μm in length and 2.16 μm in width. The image with a ruler is shown in Fig.1 to illustrate the magnification of the image.

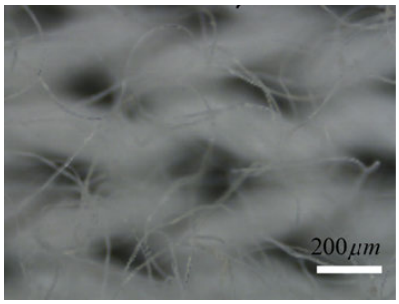

FIGURE 1. One layer of captured image with ruler.

The layer numbers and the step for acquiring sequential images have very important effects on the experimental results. Before determining the step length in the z-axis, the depth of field of the microscope was calculated by (1)

$$d_{tot} = d_g + d_p = \frac{n}{M \times NA} e + \frac{n\lambda}{NA^2} \tag{1}$$

where d_g refers to the geometric depth, d_p is the physical depth, M represents the lateral magnification of microscope, which is 143.5, NA is 0.25, n in an air medium is 1, λ is 0.55 μm, and e is the limit resolution distance, which is set to be the length of a pixel (2.16 μm).

The depth of field was calculated to be 8.86 μm. To ensure that any point on the fabric surface can find its best focal position, the captured sequential images should fully cover the depth range of the pilled fabric, and the distance between image layers should be no more than the depth of field. For the latter parameter, the distance between the image layers was set to be 8.86 μm. For the former parameter, since the height of a ball on the pilled fabric is generally 300 μm, the theoretical layer number is 34. However, considering that some balls may, in general, be relatively higher than the height value in general, the layer number was eventually set as 61 after multiple experiments with image acquisition.

Fig. 2 illustrates the parts of the captured images of these five fabrics.

B. DEPTH IMAGE RECONSTRUCTION

The main idea of image reconstruction is to calculate the depth data (z) for each point (x, y) by finding the in-focused image layer that has the maximum clearness. The key for the

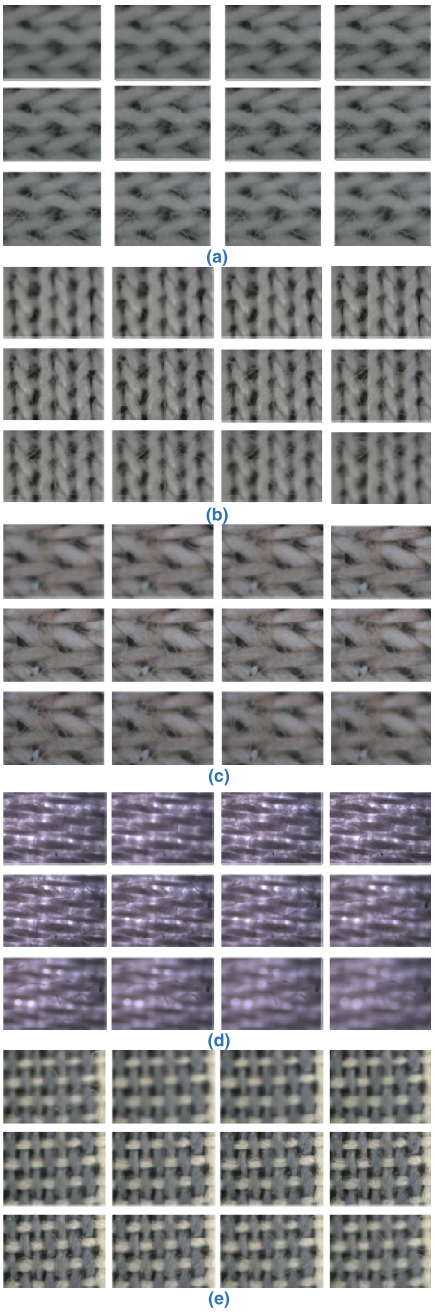

FIGURE 2. The captured images of the five samples. (a) Sample A with grade 1 pilling; (b) sample B with grade 2 pilling; (c) Sample C with grade 3 pilling; (d) Sample D with grade 4 pilling; (e) Sample E with grade 5 pilling.

algorithm is to calculate the clearness correctly. In a previous study, a clarity evaluation method was proposed based on the gradient variance of a region.

In this paper, a 7×7 sharpness window, centered with a pixel whose sharpness was to be measured, was used to assess the clearness of a certain pixel, which can be expressed as:

$$C_i(x, y) = \sum (S_i(m, n) - U_i(x, y))^2 \tag{2}$$

where $C_i(x, y)$ represents the clearness of a certain pixel (x, y) in the i-th image layer, $S_i(m, n)$ is the gradient of one pixel (m, n) within the 7×7 sharpness window, and $U_i(x, y)$ refers to the average gradient value of all pixels in the 7×7 window. The gradient $S_i(m, n)$ was calculated by the Prewitt operator.

For each fabric, 61 layers of images were captured at different focal positions. The clearness of each pixel was calculated using (1) and recorded in a 3D matrix $DCM(n, w, h)$, in which n refers to the layer number 61, w represents the pixel width of the captured image and h is the pixel height of the image. For each (x, y), by comparing the clearness $C_i(x, y)$ in all image layers ($i = 1,2, \ldots, 61$), the layer number that had the maximum clearness was the best focused layer and recorded in $I(x, y)$, which can be expressed as

$$I(x, y) = \arg\max_i DCM(i, x, y) \tag{3}$$

Assuming the maximum layer in $I(x, y)$ is $maxD$ and the minimum layer is $minD$, the depth map can be formed by (4)

$$f(x, y) = 255 - 255 \times \frac{(I(x, y) - \min D)}{(\max D - \min D)} \tag{4}$$

where $f(x, y)$ represents the gray value of pixel (x, y).

Borland C++ builder 6.0 was used to realize the depth image reconstruction algorithm. Taking the above five samples as examples, the established depth images are as shown in Fig. 3. The depth map only reflects the depth of each point, despite the colors, patterns, gloss and other appearance characteristics. Since printed patterns and colors would not change the depth of the pilled fabrics, hairiness is located above the fabric surface, and the depth value alone is the parameter that can be used to segment the hairiness and fabric surface. In the depth map, a deeper pixel color reported a greater depth.

C. HAIRINESS EXTRACTION BASED ON EDGE DETECTION AND IMAGE SEGMENTATION

In the depth image, since the hairiness is above the surface of the fabric, there is a depth discontinuity boundary between the hairiness and the fabric surface. Therefore, the segmentation algorithm based on edge detection was tried first. Taking sample four as an example, six classic edge detection methods were conducted, and the results are shown in Fig. 4.

It can be seen from Fig. 4 that depth discontinuity is more obvious at the top of the hairiness, while the depth difference between the root of the hairiness and the fabric surface is not very obvious. This difference is observed because the hairiness protrudes from the fabric surface.

The image segmentation method with the global threshold was also evaluated. Fig. 4 shows the result of the Otsu method. As seen in Fig. 5, the divided image lost partial hairiness information on the left region, while the hairiness on the right side is more complete, as shown in the circular area in the figure. This discrepancy occurs because the platform on which the microscope is placed is not an absolute horizontal plane. The right section of the fabric is higher than the left part.

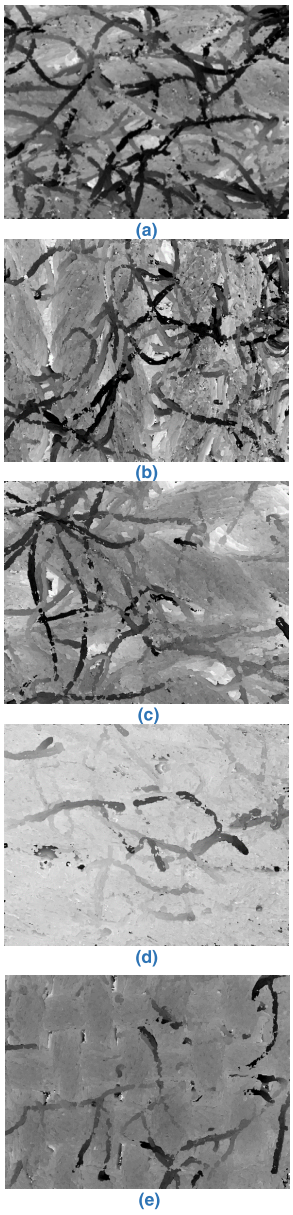

FIGURE 3. The reconstructed depth images of five samples. (a) Sample A; (b) Sample B; (c) Sample C; (d) Sample D; (e) Sample E.

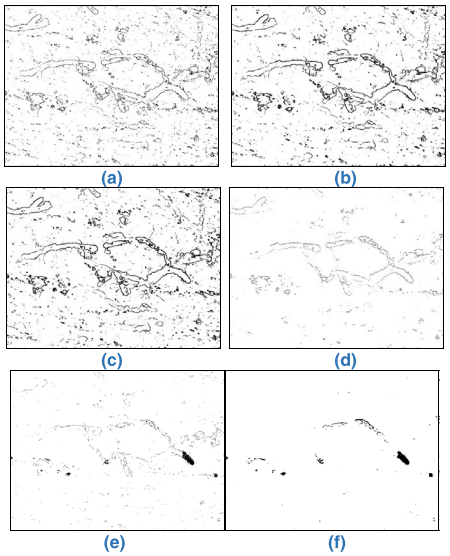

FIGURE 4. Edge detection. (a) Roberts; (b) Prewitt; (c) Sobel; (d) Canny; (e) Laplacian; (f) Log.

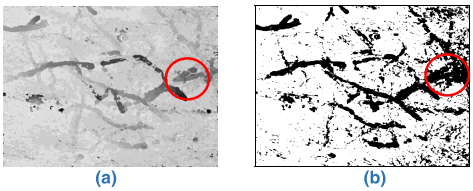

FIGURE 5. Image segmentation with the (a) depth image; (b) binary image after segmentation.

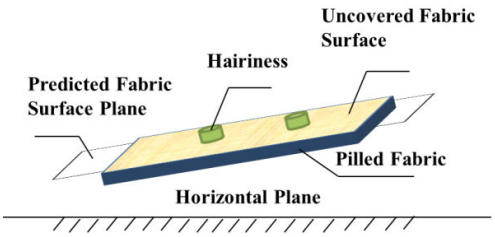

FIGURE 6. Schematic diagram of predicted fabric surface plane.

D. HAIRINESS EXTRACTION BASED ON THE PREDICTED PLANE

Based on the above, two conclusions can be drawn: (1) there is no obvious depth boundary between the hairiness root and the fabric surface since the hairiness protrudes upwards from the fabric surface; and (2) The fabric surface is not an absolute horizontal plane but, rather, a plane with an angle to the horizontal direction. Therefore, an image segmentation method based on the predicted fabric plane is proposed in this paper. In this method, we assume that the surface of the fabric is a rigid plane with a small angle to the horizontal plane. The hairiness is protruded from the plane, so the hairiness is above the fabric surface (as shown in Fig. 6).

In the area covered with hairiness, the surface depth of the fabric cannot be obtained directly from the depth image, while the surface depth of the fabric can be obtained from the depth image in the area not covered with hairiness. Therefore, a predicted fabric surface plane was established based on some base points selected within the area where the fabric surface is not covered by hairiness. The plane coordinates (x, y) and depth value (z) of each base point were then recorded. Finally, the predicted plane of the fabric was fitted using the least square method. Once the fitting reference plane of the fabric was established, the surface depth of the fabric at any position could be calculated by its coordinate value (x, y) using the predicted plane equation.

The correct selection of the base points is the key to successfully establishing the predicted plane by using the mean shift algorithm.

An over segmented method based on the mean shift algorithm was adopted is this step. The method can be illustrated as shown in Fig. 6. First, several seed points for the mean shift were selected along the detected edges; then, several local small areas were formed after the growth of each seed point with mean shift. These areas are called split pieces. Some split pieces are located on the surface of the fabric, while some are located on the hairiness area. Then, the split pieces on the surface of the fabric were extracted. Next, the spatial coordinates (x, y, z) of the fabric surface split pieces were used to establish the predicted plane via the least square method. Finally, targets above the predicted plane were extracted as hairiness. Fig. 7 shows the flow of the image segmentation methods based on the fabric surface predicted plane. In this part, the Borland C++ builder 6.0 was used to extract the hairiness.

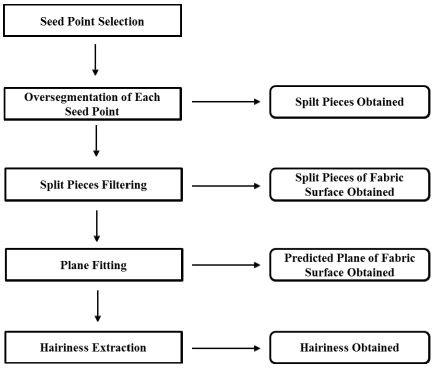

FIGURE 7. Flow chart of the hairiness extraction based on the predicted fabric surface plane.

1) SEED POINT SELECTION

As discussed above, there are depth discontinuity edges between the top of the hairiness and the fabric surface. Along both side of these edges, the seed points can be successfully selected. In a previous experiment, the Sobel operator was found to be more effective, so in this section we use a Sobel operator for edge detection.

The edge detection method will choose the pixels with the strongest local signal but ignore the contribution of their adjacent points during edge finding. Each edge pixel represents the maximum gradient of the local region: however, the adjacent points around it may also have a certain probability of becoming an edge, and their depth and gradient values are still different from the body points of the object. While these ''intermediate points'' will not be judged as edge points, they cannot be completely taken as the body area of the target. These points should instead be avoided when selecting the seed points. When the seed region is selected along both sides of the edge, in order to ensure the regions on both sides are reasonably separated, we apply the expansion algorithm to the deep discontinuity edge. The number of iterations of the expansion algorithm was set to 3.

2) SEED POINT GROWTH

Mean shift is essentially a kernel density estimation algorithm, which moves each point to the local maximum point of the density function, that is, the point with a density gradient of 0.

Let x_i, $i = 1, 2, \ldots, n$ be the known data points in 3D space. Given the multivariable kernel function $G(x)$ and the window width matrix function H with a size of $h \times h$, the mean shift vector can be expressed as:

$$m_{h,g(x)} = \frac{\sum_{i=1}^{n} x_i g\left(\left\|\frac{x-x_i}{h}\right\|^2\right)}{\sum_{i=1}^{n} g\left(\left\|\frac{x-x_i}{h}\right\|^2\right)} - x \tag{5}$$

where

$$g(x) = -k(x) \tag{6}$$

where $k(x)$ refers to the profile function.

Given the kernel function $G(x)$ and the bandwidth matrix H, the mean shift drift step is derived:

1) calculate the means hit vector $m_{h,g}(x)$.

2) assign $m_{h,g}(x)$ to x.

3) if $||m_{h,g}(x) - x|| < \varepsilon$, the loop ends; otherwise, start a new loop.

In this paper, the Epanechikov kernel function and an 8×8 window width were used in the mean shift algorithm.

In this section, Borland C++ builder 6.0 was used to realize the growth algorithm based on (5). The Fig. 8 is an enlarged view of one local area showing the selected seed points and the splits obtained after point growth, where points in the split grown from the red point are marked with red color and the split grown from the green point are marked with green color. After the growth of all seed points, all the split pieces obtained are shown in Fig. 9.

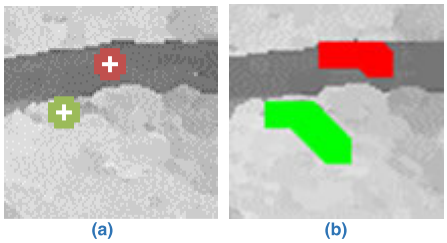

FIGURE 8. An enlarged view of one local area. (a) Two seed points; (b) Split pieces after growth of the seed points.

3) FABRIC SURFACE SPLITS EXTRACTION

To select the base points, the original splitters need to be classified and filtered. According to the depth and geometric features of the hairiness and fabric surface, a fabric surface splits extraction method based on the combination of the normal vector direction and depth value is proposed in this chapter.

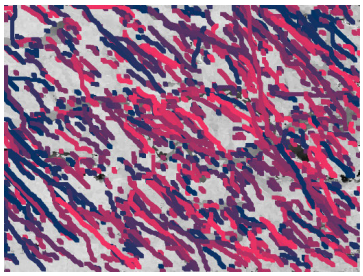

FIGURE 9. The split pieces of all seed points.

In the depth image of the pilled fabric, the hairiness protrudes upward from the fabric surface, so its geometric relationship with the fabric surface can be divided into two parts (as shown in Fig. 10). In the root area where the hairiness initially protrudes out of the fabric surface, the depth difference (d_1) between the hairiness and the fabric surface is small, while the main difference occurs in the direction of the plane normal vector. Considering that there is a slight angle between the fabric surface and the horizontal plane, the normal vector should have a small angle with the vertical direction, but it is still approximately perpendicular to the horizontal plane. However, there is a large angle between the plane's normal vector and the vertical vector in the pilling root region, which can separate the fabric surface from the hairiness connected to the surface. In the middle and top of the hairiness, the hairiness is obviously above the surface of the fabric, and the depth difference (d_2) is considerable.

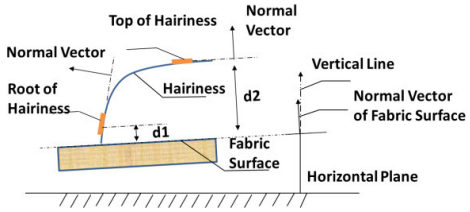

FIGURE 10. Sketches of the hairiness and fabric surface.

The geometric features of split pieces at different locations (hairiness or fabric surface) can be expressed as follows:

1) The split pieces on the fabric surface. The depth value is lower than others, and its plane normal vector is almost perpendicular to the horizontal plane.
2) The split pieces on the hairiness roots. The angles between the normal vectors of these split pieces and the vertical vector are larger.
3) The splits pieces located on the top of the hairiness. Due to the influence of gravity, the top region of hairiness is almost parallel to the fabric surface, so the normal vector of this type of piece is not different from that of the fabric surface. However, there is an obvious depth difference between them.
4) The splits pieces on the middle part of the hairiness. The normal vector and depth of this type of piece are obviously different from those of the fabric surface.
5) Split pieces with noise. Noise points are isolated points with an abnormal depth where there is an obvious depth fluctuation between them and the surrounding adjacent points. Therefore, the depth information of the split piece containing noise points will fluctuate greatly.

Since the growth of the seed points would end when encountering the edge, it is impossible for one piece to cross the fabric surface and the hairiness region. The pieces across the edge of the hairiness pixel and the fabric surface pixel will not be considered in this paper.

To summarize, three parameters can be used to distinguish the five types of split pieces, that is, the depth value, the normal vector and the depth fluctuation degree. The performance of the five types of split pieces can be summarized in Table 1.

Assuming that a split-piece named PATCH_CLOUD is given, the plane position and depth value of all pixels in the pieces are known. The gray level will be used as the depth value. The larger the gray values of the pixel (0 for black and 255 for white), the lower the depth values.

The average gray value (*gray_ave*) and gray variance (*gray_dev*) of PATCH_CLOUD can be calculated. Since the plane coordinates (x, y) and the depth value (z) of each pixel point in the pieces are known, the fitting planes ($\alpha x + \beta y + z + \gamma = 0$) of all pieces can be calculated by the least square method, and the plane normal vector (*patch_vector*), which is (α, β, 1) of the piece can be obtained.

The *threshold_dev* was used to filter the split-pieces with noisy spots, which exhibited obvious depth fluctuation. For each split piece, calculate variation coefficient by using (7), and the one of which the value of CV is above 0.15 was

TABLE 1. The geometric features of split pieces.

Location of the Split Piece	Depth Value	Normal Vector	Depth Fluctuation
On fabric surface	Small	Almost perpendicular to the horizontal plane	Not obvious
On hairiness root	Similar to fabric surface	Large angle to the horizontal plane	Not obvious
On top of the hairiness	Large	Almost perpendicular to the horizontal plane	Not obvious
On Middle part of the hairiness	Relatively large	Large angle to the horizontal plane	Not obvious
Noise	Uncertain	Uncertain	Obvious

determined as split-pieces with noisy spots.

$$CV = \frac{sqrt(gray\_dev)}{gray\_ave} \tag{7}$$

For the remaining four kinds of split pieces, the split piece located on fabric surface are almost perpendicular to the horizontal plane. The normal vector can be used to filter the split-pieces on hairiness root and on middle part of hairiness. Therefore, the angle between the normal vector $(\alpha, \beta, 1)$ and the vertical direction of all split pieces were calculated. After experience of over 400 pilled fabric images, the allowable error can be manually determined as 1.5 degrees. Thus, the split piece whose angle between the normal vector $(\alpha, \beta, 1)$ and the vertical direction above 1.5 was filtered.

After the above two steps of filtering, only two types of splits remain: the split pieces on the fabric surface and the pieces on the top of the hairiness. The main difference between these two types is the depth value. The average gray value (*gray_ave*) was the main indicator to distinguish the two kinds of split-pieces. In this part, since the average gray value (*gray_ave*) of the splits on fabric surfaces are almost gather and the average gray value (*gray_ave*) of splits on the top of the hairiness vary from the height of the hairiness, so there would be a peak on gray histogram of the remaining splits. Thus, the data segmentation method based on the histogram was used in this part to filter splits on the top of hairiness: firstly, find severa splits l local peaks in the gray histogram, and the peak declaring maximum value is considered as the gathering of fabric surface pieces; then find the nearest trough on both sides of the peak; if two troughs are found, the split-pieces between two troughs can be considered as pieces on fabric surface; if only one trough is found, the split-pieces between the trough and the peak can be considered as pieces on fabric surface.

In this section, Borland C++ builder 6.0 was used to realize the filtration process. The extracted fabric surface split pieces are shown in Fig. 11.

4) PREDICTED FABRIC SURFACE PLANE ESTABLISHMENT

In this part, two methods are used to establish the fabric surface plane: the least squares to fit the surface plane and the Hough transform to extract the surface plane.

The split piece includes a cluster of pixel points with similar depth values, so the 3D coordinates (*x, y, z*) of one split piece can be obtained from the mean value of pixels in it. The plane equation can be expressed as follows:

$$z = ax + by + c \tag{8}$$

where z represents the fabric surface depth, (x, y) refers to the plane coordinates, and a, b, and c are the coefficients. In a previous part of the paper, the z value was represented by the gray value of pixel. In this part, the gray value of each pixel is inversely converted to the layer number. Thus, the

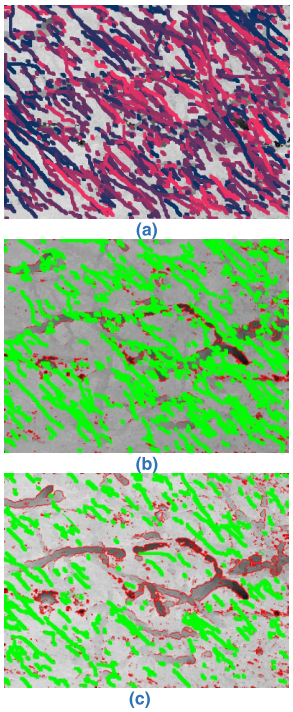

FIGURE 11. The filtered split pieces. (a) After filtering based on gray variance; (b) After filtering based on the normal vector; (c) The extracted fabric surface split pieces.

z value is represented by the number of the image layer. The fitting coefficients (a, b, c) were calculated by the least square method using the coordinates (*x, y, z*) of each fabric surface split pieces as the base points.

Let the square of the predicted plane to be S, then:

$$S = \sum_{i=1}^{n} (z_i - ax_i - by_i - c)^2 \tag{9}$$

The least square method guarantees the minimum value of S, that is:

$$\frac{\partial S}{\partial a} = 0, \quad \frac{\partial S}{\partial b} = 0, \quad \frac{\partial S}{\partial c} = 0 \tag{10}$$

The coordinates can be represented as follows:

$$\begin{cases} a\sum\limits_{i=1}^{n} x_i^2 + b\sum\limits_{i=1}^{n} x_i y_i + c\sum\limits_{i=1}^{n} x_i z_i = -\sum\limits_{i=1}^{n} x_i \\ a\sum\limits_{i=1}^{n} x_i y_i + b\sum\limits_{i=1}^{n} y_i^2 + c\sum\limits_{i=1}^{n} y_i z_i = -\sum\limits_{i=1}^{n} y_i \\ a\sum\limits_{i=1}^{n} x_i z_i + b\sum\limits_{i=1}^{n} y_i z_i + c\sum\limits_{i=1}^{n} z_i^2 = -\sum\limits_{i=1}^{n} z_i \end{cases} \tag{11}$$

The upper formula can be transformed into a matrix form:

$$\begin{bmatrix} a & b & c \end{bmatrix}^T = K^{-1}Q \tag{12}$$

Among which

$$K = \begin{bmatrix} \sum_{i=1}^{n} x_i^2 & \sum_{i=1}^{n} x_i y_i & \sum_{i=1}^{n} x_i z_i \\ \sum_{i=1}^{n} x_i y_i & \sum_{i=1}^{n} y_i^2 & \sum_{i=1}^{n} y_i z_i \\ \sum_{i=1}^{n} x_i z_i & \sum_{i=1}^{n} y_i z_i & \sum_{i=1}^{n} z_i^2 \end{bmatrix} \tag{13}$$

$$Q = \begin{bmatrix} -\sum_{i=1}^{n} x_i \\ -\sum_{i=1}^{n} y_i \\ -\sum_{i=1}^{n} z_i \end{bmatrix} \tag{14}$$

In the Hough transform method [14], the plane in (8) is transformed into the 3-dimensional Hough space (θ, φ, ρ). The plane in the Hough transform can be given by a point $\vec{p}$ on the plane, the normal vector $\vec{n}$, which is perpendicular to the plane, and the distance ρ between the plane and the original point, which can be expressed as follows:

$$\rho = \vec{p} \cdot \vec{n} = p_x n_x + p_y n_y + p_z n_z \tag{15}$$

The expansion of the normal vector $\vec{n}$ can be expressed as follows:

$$\vec{n} = \begin{bmatrix} n_x \\ n_y \\ n_z \end{bmatrix} = \begin{bmatrix} \cos(\theta)\sin(\varphi) \\ \sin(\theta)\sin(\varphi) \\ \cos(\varphi) \end{bmatrix} \tag{16}$$

where θ is the angle of the normal vector on the xy-plane and φ is the angle between the xy-plane and the normal vector in z-axis. To find planes in a point set, one calculates the Hough transform for each point. By voting in the 3-dimensional Hough space (θ, φ, ρ), the extreme point of each parameter can be obtained; thus, the best extracted predicted plane can be established.

By using the equation of the predicted plane, we can calculate the depth value of the fabric surface at any plane position. The depth information can be used as the local threshold to segment hairiness from fabric background. It is worth noting that when establishing the depth image, the layer number [0,60] had been projected into the grayscale space [0,255]. Since the step length of platform movement is fixed, the depth difference between image layers is fixed. Assuming the depth value of coordinate position (x, y) of fabric surface is $z(x, y)$, which can be calculated through the equation of the predicted plane. and depth value (which is represented in grayscale) of the corresponding pixel (x, y) on the depth image is I (x, y), then the height of the hairiness pixel $H_s(x, y)$ can be calculated as follows:

$$H_s(x, y) = \begin{cases} 0 & if\ I_s(x, y) <= Z(x, y) \\ I_s(x, y) - Z(x, y) & if\ I_s(x, y) > Z(x, y) \end{cases} \tag{17}$$

For a planar pixel (x, y), if $H_s(x, y)$ is larger than zero, it can be considered as hairnesses, otherwise fabric surface. Sort the I_s of all pixels, then the maximum value I_s_max and the minimum value I_s_min can be obtained. The projection of $I_s(x, y)$ into grayscale space is expressed as follows:

$$f(x, y) = 255 - 255 \times \frac{(I_s(x, y) - I_s\_\min)}{(I_s\_\max - I_s\_\min)} \tag{18}$$

$f(x, y)$ represents the image gray value, and the extracted image is shown in Fig.12.

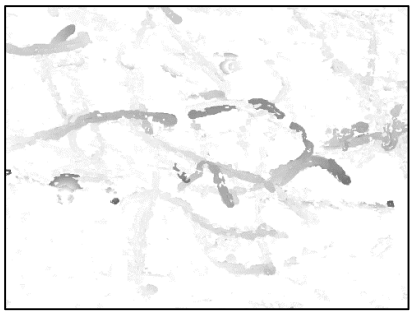

FIGURE 12. The extracted hairiness.

III. RESULTS AND DISCUSSION

To verify the correctness of the proposed algorithm, the depth images of five fabric samples, Sample A to Sample E, were used for statistical experiments in this paper.

A. SIGNIFICANCE ANALYSIS OF THE FABRIC SURFACE

The proposed image segmentation algorithm is based on the assumption that the fabric surface is a plane with a slight inclination angle to the horizontal plane. To test the hypothesis, a significance analysis of the fabric surface was conducted. In the hypothesis, the depth value (z) of each point on the fabric surface is supposed to have a linear relationship with the spatial coordinates (x, y). Thus, the three-dimensional coordinates (x, y, z) of the fabric surface split pieces were used as test values to verify the significance of the plane. The linear relationship is shown as follows:

$$\begin{cases} z_i = ax_i + by_i + c + \varepsilon \\ \varepsilon \sim N(0, \sigma^2) \end{cases} \tag{19}$$

The regression coefficients (both a and b) will be tested. If they are both zero, then the linear relationship is considered not significant; otherwise, the linear relationship is considered to be significant. Thus, the following hypothesis can be put forward:

$$H_0 = a = b = 0 \tag{20}$$

The F test was used to verify the test statistics for the hypothesis H_0. The observation value F was calculated as follows:

$$F = \frac{\sum_i (\hat{z}_i - \bar{z})^2 / m}{\sum_i (\hat{z}_i - z_i)^2 / (n - m - 1)} \tag{21}$$

$$\hat{z}_i = ax_i + by_i + c \tag{22}$$

TABLE 2. The significance test of the fabric surface.

Sample	Predicted Plane	Degree of Freedom	Critical Value	F ValueValue
1	$z = -0.0053x + 0.0008y + 27.5$	102	3.09	24.22
2	$z = -0.0021x + 0.0012y + 29.8$	122	3.07	15.63
3	$z = 0.0642x + 0.004y + 24.7$	239	3.04	16.57
4	$z = 0.0015x + 0.001y + 27.4$	392	3.03	23.19
5	$z = -0.001x + 0.0031y + 8$	139	3.06	13.24

where $\hat{z}_i$ is the predicted depth value, $\bar{z}_i$ represents the average value, m is the number of variables (set to be 2 in this experiment), and n is equal to the amount of test data. For a given significance level α, the test rule can be described as: If $F \geq F_{1-\alpha}(m, n-m-1)$, reject H_0.; otherwise, accept H_0.

Through deduction of (12) with the coordinates of the all pieces, the values of the coefficients a, b and c were obtained. Let the significance level α be 0.01, where the predicted plane equation and the F value test results of the five samples are shown in Table 1.

It can be seen from Table 2 that the F values of all five fabric samples are greater than the critical value, so it can be concluded that the depth values of the fabric surface have a significant linear relationship to the plane coordinates; thus, the assumption that the fabric surface is a plane is reasonable.

B. ACCURACY TEST OF THE PREDICTED FABRIC SURFACE PLANE

To verify the accuracy of the established fabric surface plane, 200 pixels scattered on the fabric surface area were manually and randomly selected from the five fabric sample depth images. The 200 pixels were not used when establishing the predicted plane. The depth values of the corresponding pixels obtained by manual focusing were used as the true data for comparison. The depth values obtained by using the predicted plane were used as the predicted data. The residual values between the predicted depth value and the true depth values were calculated and used to verify the prediction ability of the plane equitation.

For each image there are two sets of data: one set is the predicted data $\hat{z}_i (i = 1, 2, \ldots, 200)$, and the other set is the true data $z_i (i = 1, 2, \ldots, 200)$. The residual value was calculated according to (23).

The least square method and the Hough transform method were both used to establish the predicted fabric surface plane. With the least square method, the plane that has the minimum sum of the distance of all points is expected to be the fitted predicted plane, while with the Hough transform, the plane that receives the most votes is expected to be the extracted predicted plane. In this part, the residual examination was conducted on the predicted plane by using the least square method and the Hough transform method. Fig. 13 shows the residual diagram of the observation point. It can be seen from the diagram that the fluctuation range is essentially stable, and

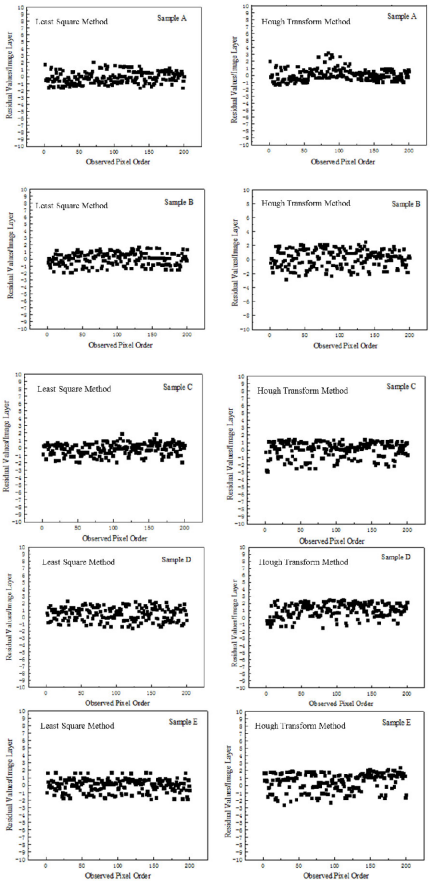

FIGURE 13. Residual plots of the five samples.

most of the residual values of the five samples obtained with the two methods are between -3 μm to 3 μm. The errors may be caused by the discontinuous capture of image layers. The series of image layers were captured at each step as the stage moved along the z-axis. The calculated focal position may not exactly be the best-focused position, but it is the position where the captured image layer has the best clearness. Thus, errors exist between the depth values calculated based on the sequential images and the real ones. Furthermore, from images in Fig. 2 we can see that there are complicated textures on fabric surface such as the yarn twist and the interlace of warp and weft yarns, which makes the hairiness extraction more difficult. In this manuscript, the fabric surface was

simplified as a rigid plane, which can be fitted by several base points on fabric surface. Hairiness above the predicted surface were extracted. This would also cause some errors, however, the depth differences between hairiness and fabric surface are far more significant than the depth differences on fabric surface caused by twisting and buckling of yarns. The depth differences between the two neighboring layers is 8.86 μm. The estimated standard error (SEE) value in the micron-unit of the five samples are shown in Table 3. It can be seen from Table 2 that the SEE values of the five samples are all approximately 1.5 μm, which are all smaller than the field depth of the microscopic system, which is 8.86 μm. Therefore, the depth estimation errors of the predicted plane are acceptable. It can also be seen from Table 3 that for sample A and sample D, the SEE values obtained with the Hough transform method are smaller than those with the obtained with the least square method. For other samples, the SEE values obtained with the least square method are better. In fact, the residual examination differences between the two methods are not substantial. Considering that the

TABLE 3. Residual analysis of the predicted fabric surface plane.

SEE/μm	A	B	C	D	E
Hough Transform Method	1.43	1.88	1.96	1.29	1.76
Least Square Method	1.49	1.59	1.38	1.96	1.51

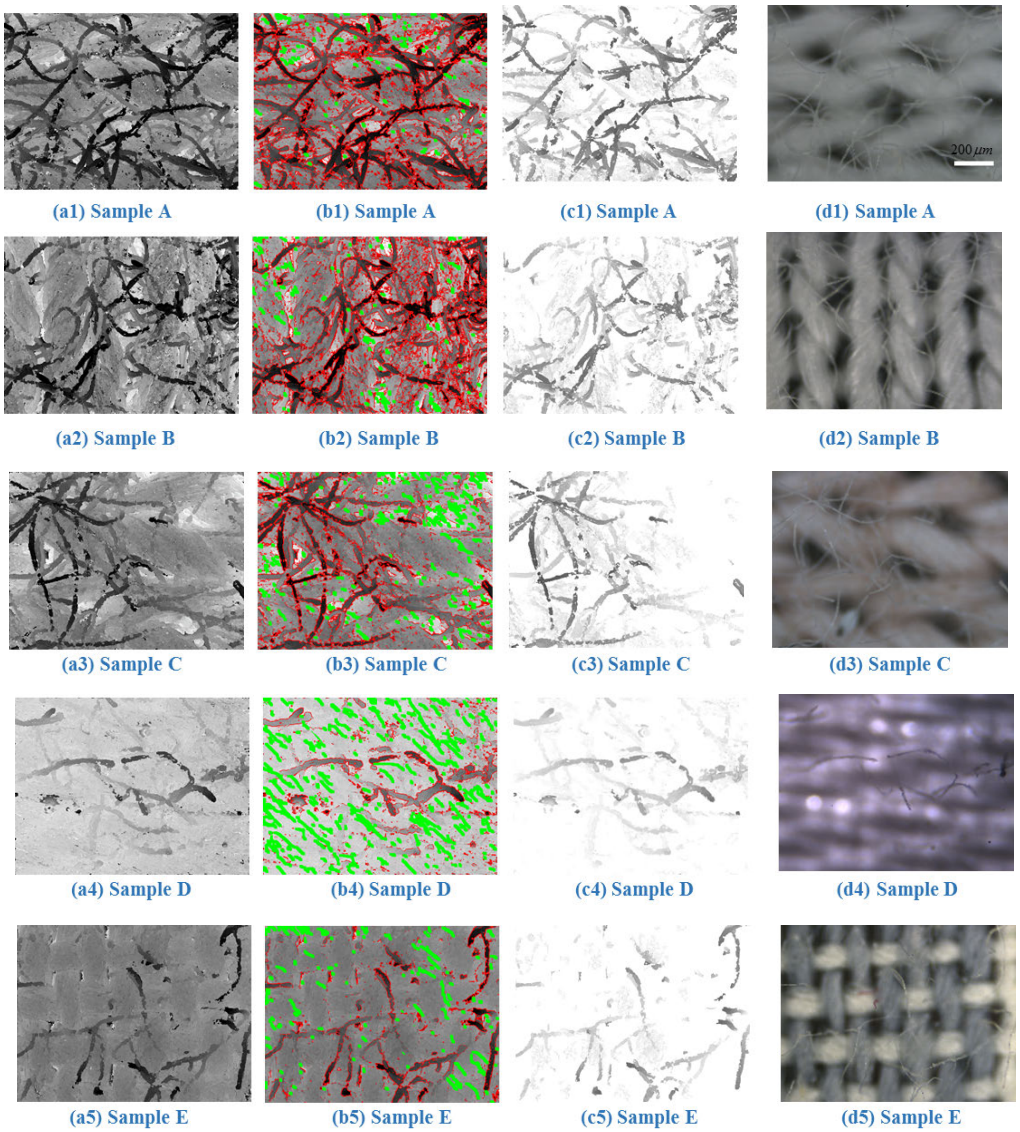

FIGURE 14. The procedure of hairiness extraction for the five samples. (a) The depth image of the five samples; (b) the extracted fabric surface split pieces of the five samples; (c) the extracted hairiness images of five samples; (d) The captured image layer of the five samples.

voting process in Hough transform would require relatively more computation time, the least square method was finally adopted to establish the predicted plane.

$$e = \hat{z} - z \tag{23}$$

C. THE EXTRACTED HAIRINESS IMAGES BASED ON THE PREDICTED FABRIC SURFACE PLANE

The extracted hairiness images of the fabric samples are shown in Fig. 14. Fig. 14(d) illustrates one of the captured image layers of corresponding fabric sample. It can be seen from the diagram that the extracted fabric surface pieces are uniformly dispersed within the fabric surface region without crossing the boundary between the hairiness and the fabric surface. The segmented images conclude the complete information of the hairiness, and the remaining depth information is given through grayscale. The method of hairiness extraction based on the predicted plane is effective and accurate.

IV. CONCLUSION

This paper provided a method of extracting hairiness from the fabric background based on the predicted fabric surface plane. The depth value of the fabric surface was taken as the absolute index to segment the hairiness and the fabric surface. Targets that were above the fabric surface were considered to be hairiness. To predict the depth information of the fabric surface where it was covered with hairiness, a predicted fabric surface plane was established based on several base points using the least squares estimation. The significance testing and the residual examination demonstrated the assumption that the horizontal coordinates of the fabric surface points have a significantly linear relationship to the depth values, and the predicted plane can correctly calculate the depth value (z) of the fabric surface at any plane position (x, y). The extracted hairiness images of the five samples showed that this method could effectively extract the hairiness from the fabric surface.

REFERENCES

[1] D. Wang, J. Barber, W. Lu, and M. Thouless, "Use of wavelet analysis for an objective evaluation of the formation of pills in nonwoven fabrics," *J. Ind. Textiles*, vol. 49, no. 5, pp. 663–675, Nov. 2019.
[2] V. M. Mayekar and R. P. Nachane, "Fabric pilling-objective measurement system," *Indian J. Fibre Text. Res.*, vol. 41, pp. 338–343, Sep. 2016.
[3] R. Furferi, M. Carfagni, L. Governi, Y. Volpe, and P. Bogani, "Towards automated and objective assessment of fabric pilling," *Int. J. Adv. Robotic Syst.*, vol. 11, no. 10, p. 171, Oct. 2014.
[4] C. Yang, C. J. Lin and W. J. Chen, "Using deep principal components analysis–based neural networks for fabric pilling classification," *Electronics*, vol. 8, no. 5, p. 474, Apr. 2019.
[5] S. Guan, W. Li, J. Wang, and M. Lei, "Objective evaluation of fabric pilling based on data-driven visual attention model," *Int. J. Clothing Sci. Technol.*, vol. 30, no. 2, pp. 210–221, Apr. 2018.
[6] Z. Deng, L. Wang, and X. Wang, "An integrated method of feature extraction and objective evaluation of fabric pilling," *J. Textile Inst.*, vol. 102, no. 1, pp. 1–13, Jan. 2011.
[7] C.-L. Lee and C.-J. Lin, "Integrated computer vision and type–2 fuzzy CMAC model for classifying pilling of knitted fabric," *Electronics*, vol. 7, no. 12, p. 367, Dec. 2018.
[8] M. Eldessouki and M. Hassan, "Adaptive neuro-fuzzy system for quantitative evaluation of woven fabrics' pilling resistance,," *Expert Syst. Appl.*, vol. 42, no. 4, pp. 2098–2113, Mar. 2015.
[9] L. Techniková, M. Tunák, and J. Janáček, "New objective system of pilling evaluation for various types of fabrics," *J. Textile Inst.*, vol. 108, no. 1, pp. 123–131, Jan. 2017.
[10] P. Xu, X. Ding, R. Wang, and X. Wu, "Feature-based 3D reconstruction of fabric by binocular stereo-vision," *J. Textile Inst.*, vol. 107, no. 1, pp. 12–22, Jan. 2016.
[11] L. Wang, W. Ouyang, W. Gao, and B. Xu, "Instrumental evaluation of fabric abrasive wear using 3D surface images," *J. Textile Inst.*, vol. 108, no. 5, pp. 846–851, May 2017.
[12] X. Zhang, Z. Liu, M. Jiang, and M. Chang, "Fast and accurate autofocusing algorithm based on the combination of depth from focus and improved depth from defocus," *Opt. Express*, vol. 22, no. 25, p. 31237, Dec. 2014.
[13] M. Moeller, M. Benning, C. Schonlieb, and D. Cremers, "Variational depth from focus reconstruction," *IEEE Trans. Image Process.*, vol. 24, no. 12, pp. 5369–5378, Dec. 2015.
[14] D. Borrmann, J. Elseberg, K. Lingemann, and A. Nüchter, "The 3D Hough transform for plane detection in point clouds: A review and a new accumulator design," *3D Res.*, vol. 2, no. 2, p. 3, Jun. 2011.

CHAO ZHI was born in Xi'an, Shaanxi, China, in 1986. He received the B.S. and M.S. degrees in textile engineering from Xi'an Polytechnic University, Xi'an, in 2012, and the Ph.D. degree in textile engineering from Donghua University, Shanghai, China, in 2017.

Since 2017, he has been an Associate Professor with the School of Textile Science and Engineering, Xi'an Polytechnic University. In 2016, he was funded by the China Scholarship Council (CSC) and performed research for the Commonwealth Scientific and Industrial Research Organization (CSIRO) Geelong, Australia, for one year. He is the author of more than 20 articles. His research interests include image processing of textile composites and finite element simulations of composite interfacial bond properties.

Dr. Zhi is a member of the China Textile Engineering Society. He is hosting several scientific research projects that are supported by the National Natural Science Foundation of China, Science and Technology Project of Shaanxi, China and the Scientific Research Program of Shaanxi Provincial Education Department. He is a reviewer of several journals, such as *Materials and Design, RSC Advances*, and the *Textile Research Journal*.

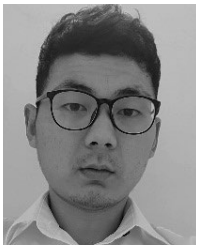

ZHONG-YUAN GAO was born in Luoyang, Henan, China, in 1996. He received the B.S. degree in textile engineering from Xi'an Polytechnic University, Shaanxi, China, in 2019, where he is currently pursuing the M.S. degree with the School of Textile Science and Engineering.

In 2019, he published his graduate thesis, Algorithm study of a semi-automatic measuring system for fiber fineness. His main research interests include modern textile techniques, computer vision, and textile engineering.

Mr. Gao's awards and honors include the excellent award of the vocational skills competition and the outstanding class cadre award of Xi'an Polytechnic University.

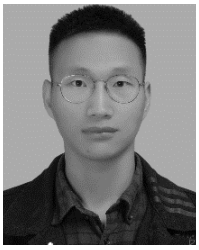

GUAN-LIN WANG was born in Lingbao, Henan, China, in 1995. He received the B.S. degree in textile engineering from Xi'an Polytechnic University, Shaanxi, China, in 2018, where he is currently pursuing the M.S. degree with the School of Textile Science and Engineering.

From 2018 to 2019, he worked as an Assistant with the Graduate Student Union, Xi'an Polytechnic University. His research interests include 3D modeling of nonwovens, machine learning, and textile image analysis.

Mr. Wang was a recipient of the outstanding students' award at Xi'an Polytechnic University and the 2019 Leoch Scholarship.

MENG-QI CHEN was born in Shangluo, Shanxi, China, in 1997. She received the B.S. degree in textile engineering from Xi'an Polytechnic University, Shaanxi, China, in 2019, where she is currently pursuing the M.S. degree with the School of Textile Science and Engineering.

From 2018 to 2019, she worked as an Assistant with the Graduate Office, Xi'an Polytechnic University. Her research interests include fabric surface image analysis and textile image analysis.

Ms. Chen was a recipient of the National Encouragement Scholarship.

WEI FAN was born in Yulin, Shaanxi, China, in 1986. He received the B.S. and M.S. degrees in textile engineering from Xi'an Polytechnic University, Xi'an, China, in 2010, and the Ph.D. degree in textile engineering from Tianjin Polytechnic University, Tianjin, China, in 2015.

Since 2015, he has been an Associate Professor with the School of Textile Science and Engineering, Xi'an Polytechnic University. In 2017, he was funded by the China Scholarship Council (CSC) and was a one-year post doctor in mechanical engineering at the University of North Texas, USA. He is the author of more than 22 articles. His research interests include structure-function integrated textile composites, manufacturing and applications of advanced textile composites, and preparation and properties of functional fibers and smart wearable fabrics.

Dr. Fan is a member of the China Composite Society. He is hosting several scientific research projects supported by the National Natural Science Foundation of China, Science and Technology Project of Shaanxi, the Natural Science Foundation of Shaanxi province, and the Science and Technology Project of China Textile Industry Federation. He is a Reviewer of several journals, such as *Materials and Design, Polymer Degradation and Stability*, and *Polymer Composites*.

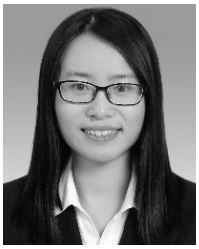

LING-JIE YU (Member, IEEE) was born in Jingdezhen, Jiangxi, China, in 1990. She received the B.S. and Ph.D. degrees in textile engineering from Donghua University, Shanghai, China, in 2011 and 2017, respectively.

Since 2017, she has been an Associate Professor with the School of Textile Science and Engineering, Xi'an Polytechnic University, Xi'an, China. She is the author of more than ten articles. Her research interests include 3D modeling of textile material microstructures and morphological measurements of fabrics, yarns, and fibers using image analysis.

Dr. Yu was a member of China Textile Engineering Society. She has been hosting the project of the Shaanxi Natural Science Fund, since January 2019. She is a Reviewer of several journals, such as *Textile Research Journal*.